Gallium-isotope fine structure of impurity modes due to defect complexes in GaAs

D. N. Talwar
Department of Marine Sciences, Texas A&M University at Galveston, P.O. Box 1675, Galveston, Texas 77553

M. Vandevyver
Department de Physico-Chimie, Commissariat à l'Energie Atomique, Centre d'Etudes Nucléaires de Saclay, Boîte Postale No. 2, 91191, Gif-sur-Yvette, Cedex, France

K. K. Bajaj
Avionic Laboratories, Air Force Wright Aeronautical Laboratories/AADR, Wright Patterson Air Force Base, Ohio 45433

W. M. Theis
University Research Center, Wright State University, Dayton, Ohio 45435
(Received 14 January 1986)

A comprehensive Green's-function calculation was performed in order to understand the recent high-resolution Fourier-transform infrared absorption (FTIR) data of localized vibrational modes (LVM's) due to isolated (Si_{Ga} donor, B_{Ga} isoelectronic, Si_{As}, Li_{As}, B_{As} acceptor) and pair (Si_{Ga}-Si_{As}, Si_{Ga}-As-Li_{Ga}) defects in GaAs. For the defect centers with T_d, C_{3v}, C_s, and C_{2v} symmetries, we have considered simple perturbation models using mass changes at the impurity sites and nearest-neighbor (NN) force-constant changes between impurity-host atoms. For the host GaAs, all the involved Green's-function matrix elements are numerically evaluated by incorporating "phonons" generated by an eleven-parameter rigid-ion model (RIM11) fitted to the neutron data of phonon dispersions. After analyzing nearly *eighty* cases of LVM's in *fifteen* elemental and compound semiconductors, we strongly argue that there exists a close relationship between the *force perturbation* and the variation of the *covalency of the bond.* Based on simple physical reasonings we have proposed empirical relationships which provide correction to the force constants for closest mass isoelectronic (i), donor (d^+), and acceptor (a^-) impurities carrying static charges. Such trends of force variation are found to be important not only in studying the pair defect vibrations (Si_{Ga}-Si_{As}, Li_{Ga}-Si_{Ga}) but also in understanding the possibility of the occurrence of boron antisite (B_{As}^-) defects in GaAs. Using the force perturbation parameter obtained from the T_d case, and considering *two* Ga (^{69}Ga, ^{71}Ga) isotopic masses in different NN configurations with C_{3v} and C_{2v} symmetries, we have qualitatively explained the recent Ga-isotopic fine structure of LVM's due to B_{As}^-. To understand the origin of the 367- and 369-cm^{-1} bands observed in Si-doped GaAs samples, *two* perturbation models each involving one ^{28}Si and a *self-antisite* defect are proposed and evaluated in terms of the Green's-function theory. The results are compared and discussed with the existing theoretical and experimental data.

I. INTRODUCTION

The increasing technological importance of defects in II-VI and III-V compounds for optical devices has stimulated considerable interest in the electronic[1–4] and vibrational[5–7] (phonon) properties. Despite numerous recent experimental efforts using electron paramagnetic resonance[8,9] (EPR), electron-spin resonance[10] (ESR), and deep-level transient spectroscopy[11–14] (DLTS), there is still much controversy and mystery surrounding the identification of native defects (e.g., vacancies, self-interstitials, and antisites) which produce nonstochiometry and deep localized levels. An alternative way of investigating the behavior of impurity centers in semiconductors is to study the vibrational spectrum through optical [infrared (ir) absorption and Raman scattering] experiments. The electrical data has been used in conjunction with the expected defect symmetries to assign the *sites* of defects responsible for the observed absorption bands in the optical experiments.[15–17] In most of the earlier studies,[5–7] standard grating spectrometers were used with a spectral resolution of the order of $\sim$0.5–1 cm^{-1} for the spectral range $\sim$200–700 cm^{-1}. Recently, a significant increase in the resolution[10] ($\sim$0.04 cm^{-1}) of the instrumental probe has been achieved and conclusions drawn from the low-resolution data are more rigorously tested and in some cases put on much firmer ground.

Of particular interest in recent years have been the vibrational properties of C and Si in GaAs.[19–24] Aside from their technological importance, an additional reason for studying these systems is to understand the role of amphoteric defects (e.g., group-IV atoms) in III-V compounds. It has been well established that ^{28}Si substituted on a Ga site ($^{28}Si_{Ga}$) in GaAs, acts like a *donor* (d^+) and

is responsible for the localized vibrational mode (LVM) observed near 384 cm^{-1}, while Si substituted on an As site ($^{28}Si_{As}$) is an acceptor (a^-) and accounts for a mode detected[5–7] near 399 cm^{-1}. Besides forming nearest-neighbor (NN) "donor-acceptor" pairs[22,25–30] in III-V—compound semiconductors, silicon also enters into a number of complexes,[5–7] especially when other impurities[31–34] (e.g., Li, B, etc.) are present. Previous ir measurements with low resolution[19–22] have revealed that the full width at half maximum (FWHM) of the absorption line associated with $^{28}Si_{As}$ is significantly higher (~ 2.2 cm^{-1}) than that for $^{28}Si_{Ga}$ (~ 1.5 cm^{-1}). The width of such a band actually depends on the lifetime of the localized oscillator in its first-excited state and also upon the inhomogenities in the crystal. Using a Fourier-transform ir (FTIR) spectrometer with an instrumental resolution of 0.06 cm^{-1}, Theis *et al.*[15] have provided experimental justification to the above argument by resolving the $^{28}Si_{As}$ transition into at least three lines. The explanation of the structure for the $^{28}Si_{As}$ bands is the reduction in the symmetry and small frequency shifts produced by the two naturally occurring Ga isotopes [^{69}Ga (60.4%) and ^{71}Ga (39.6%)] distributed in different ways over the four NN sites to the silicon impurity.

In contrast to the *two* observed LVM's (localized vibrational modes) due to isolated Si defects in GaAs, the ir measurements in ^{12}C-doped samples have demonstrated the occurrence of only one vibrational mode[23,24] near 582.4 cm^{-1}. An isotopically shifted band near 561.2 cm^{-1} has also been detected due to ^{13}C. Chemical analyses of the samples provided no information about the lattice location of the impurity atoms. Photoluminescence[35] and other measurements[34] have, however, shown that carbon is a *shallow* acceptor with a ground state approximately 26 meV above the top of the valence band. Quite recently, the observed LVM due to ^{12}C in GaAs has been resolved into *four* (or perhaps *five*) overlapping bands with high-resolution FTIR spectroscopy.[15] Comparison with the $^{28}Si_{As}$ case has suggested that the mode at 582.4 cm^{-1} should be attributed to the $^{12}C_{As}$ acceptor and the fine structure arises from the *two* Ga isotopes in different NN configurations.

The first observation of absorption due to boron in GaAs was reported by Newman *et al.*[23] Besides the observed lines at 540 and 517 cm^{-1} due to isoelectronic $^{10}B_{Ga}$ and $^{11}B_{Ga}$ defects, *two* additional lines at 628 and 601 cm^{-1} were also observed and designated as the B(2) centers.[31–33] Various arguments were presented to show that the B(2) defect has T_d symmetry and has Ga NN's, implying that the center is either a B_{As} antisite defect or a B_{int} boron atom in one of the tetrahedral interstitial sites. Recent analyses have led Woodhead *et al.*[34] to believe that the B(2) centers are $^{10}B_{As}$, $^{11}B_{As}$ antisite defects which have been confirmed by the observations[14] of NN Ga isotopic effects similar to Si_{As} and C_{As}.[15]

The splitting patterns of C_{As} and Si_{As} defects in GaAs have been analyzed recently in the framework of the Bethe-lattice and molecular-type models[37,38] of the defect interacting with its immediate neighbors. Using the simplest two-parameter force model for the host lattice, Leigh and Newman[37] have argued that the observed structure can be approximated by the calculated shifts if one increases the bend-stretch force-constant ratio at the ^{12}C impurity site.

We use here a more sophisticated Green's-function technique to study not only the NN isotopic shifts of LVM's due to B_{As} antisite defects, but also to understand the vibrational properties of some impurity complexes (e.g., Si-Si, Li-Si, etc.) in GaAs. The method[39,40] emphasizes primarily the delineation of chemical trends and the attainment of a simple physical understanding of the bonding situation through the general magnitude of the impurity-host parameters.[41] Starting with a brief outline of possible realistic methods, we will present, in Secs. II A–II C, a general Green's-function theory to study the vibrations of impurity complexes with a maximum of three substitutional defects in semiconductors. In addition to the mass changes at the impurity sites, we assume that the force-constant variations about the defects are significant only up to the first NN's. We do not consider perturbations in the Coulomb interactions since their long range would render the Green's-function approach intractable. To simplify numerical calculations, the use of group theory is outlined in Sec. II D and explicit expressions for the impurity modes are derived for general cases with defect centers of C_{3v}, C_{2v}, and C_s symmetries. Numerical calculations are made for single substitutional defects and the trends of force variations due to charged impurities are analyzed in Sec. III A. The splitting patterns of LVM's due to NN Ga isotopes for B defects on the As sublattice are studied in Sec. III B. The vibrational properties of pair defects are analyzed in Secs. III C–III D and compared with the existing experimental data. The results are discussed in Sec. IV, with concluding remarks presented in Sec. V.

II. THEORETICAL CONSIDERATIONS

To extract the nature of impurity-host bonding in semiconductors from the existing optical data, two equally reliable theoretical efforts have been made in recent years: (a) A *microscopic analysis* based on a local-density-functional approach: with the use of ionic pseudopotentials, the phonon energies for perfect or imperfect systems can be determined from *first principles*.[42] (b) A *macroscopic analysis* based on the general treatment of the lattice dynamics in terms of interatomic forces: with the use of the Green's function for the perfect or imperfect lattice, the displacement response to the sinusoidal driving forces may be estimated.[43–46] It is worth mentioning that the former type of calculation requires heavy computational work for isoelectronic defects and presumably it would be even more cumbersome for charged defects. Except for the only existing *ab initio* calculation[42] in *Ga*As:Al, the nature of impurity-host bonding has yet to be extracted by first principles for donors or acceptors in semiconductors. On the other hand, the Green's-function theory has been successfully applied over the last several years to understand the vibrational properties of imperfect solids,[43–46] including the impurity modes, impurity-induced ir absorption,[47–49] Raman scattering,[50] phonon sidebands, etc. The advantage of the second technique

over the first is that it allows the coupling of the vibrations of the defect to the bulk crystal, and one can really visualize which types of vibrational modes remain localized around the defect. A comprehensive account of the dynamical properties of imperfect lattices using Green's-function techniques has been discussed in several review articles, monographs, and books.[39,40] The discussion here is thus very brief for the purpose only of establishing the notation to be used throughout the paper.

A. Green's-function method

In the harmonic approximation, the lattice dynamics of the perfect crystal in Green's-function notation is given by[39]

$$(\underline{M}\omega^2-\underline{\Phi})\underline{G}(\omega)=\underline{1}\ , \tag{1}$$

where ω is the phonon frequency, $\underline{M}$ is the diagonal matrix containing the masses of the constituent atoms M_κ ($\kappa=1,2$), $\underline{1}$ is the unit matrix, $\underline{\Phi}$ is the force-field matrix, and $\underline{G}(\omega)$ is the lattice Green's-function matrix. The eigenfrequencies of the host system can be easily found by solving the equation

$$\det(\underline{1}\omega^2-\underline{D})=\det\underline{G}^{-1}(\omega)/\det\underline{M}\ , \tag{2}$$

where $\underline{D}=\underline{M}^{-1/2}\underline{\Phi}\,\underline{M}^{-1/2}$ is called the dynamical matrix. The eigenvectors of each mode are considered to have a sinusoidal spatial dependence allowing a unique wave vector $\mathbf{q}$ to be associated with each mode frequency. The component form of the perfect-lattice Green's-function matrix is defined as

$$G_{\alpha\beta}(l\kappa;l\kappa':\omega)=\frac{1}{N(M_\kappa M_{\kappa'})^{1/2}}\times\sum_{\mathbf{q},j}\frac{e_\alpha(\kappa\,|\,\mathbf{q}j)e^*_\beta(\kappa'\,|\,\mathbf{q}j)}{\omega^2-\omega^2(\mathbf{q}j)}\times\exp\{i\mathbf{q}\cdot[\mathbf{x}(l\kappa)-\mathbf{x}(l'\kappa')]\}\ , \tag{3}$$

where N denotes the number of wave vectors $\mathbf{q}$ in the first Brillouin zone, $\mathbf{x}(l\kappa)$ is the equilibrium position vector of atom $l\kappa$, and $e_\alpha(\kappa\,|\,\mathbf{q}j)$ are the components of the eigenvector for the mode frequency $\omega(\mathbf{q}j)$. For each eigenvalue, the eigenvectors satisfy the familiar orthogonality and closure relations.[39]

If $\underline{P}$ is the perturbation on the dynamical matrix of the host lattice, then the Green's-function matrix for the imperfect solid $\underline{U}$ is defined as

$$(\underline{M}\omega^2-\underline{\Phi}-\underline{P})\underline{U}(\omega)=\underline{1}\ , \tag{4a}$$

or, equivalently,

$$(\underline{I}-\underline{G}\,\underline{P})\underline{U}(\omega)=\underline{G}\ , \tag{4b}$$

with the perturbation matrix

$$\underline{P}=-\Delta\underline{M}\omega^2+\Delta\underline{\Phi}\ . \tag{4c}$$

Here, $\Delta\underline{M}$ and $\Delta\underline{\Phi}$ are the mass-change and force-constant-change matrices. To make the problem tractable, $\underline{P}$ is usually assumed to be very localized around the defect. One therefore needs to solve the small subblock of Eqs. (4) corresponding to the nonzero elements of the perturbation matrix.

B. Bulk phonons

As discussed in Sec. II A, the numerical calculation of the lattice Green's function [Eq. (3)], and thereby the defect properties, requires a detailed knowledge of phonon energies and eigenvectors of the host crystal from a reliable phenomenological model. In the harmonic approximation, invariance of potential energy with respect to rigid-body translations, rotations, and symmetry operations of the crystal lattice results in only *two* NN parameters (A,B) needed to describe the lattice dynamics of diamond- or zinc-blende-type crystals. However, the calculations by Grimm *et al.*[43] based on this model failed to fit the measured phonon dispersion curves of GaAs.[51] This suggests the need for elaborate force models involving interaction with more distant neighbors. We consider here an eleven-parameter rigid-ion model[52] (RIM11) to treat the lattice dynamics of both perfect and imperfect GaAs. This RIM11 includes short-range interactions up to and including second NN (2NN) and long-range Coulomb effects arising from the electrostatic interaction. The choice of the model will facilitate comparison of our results with the analogous ones obtained earlier in other II-VI and III-V compounds.[45–47]

In the RIM11, the quantities of interest for our calculations are the force-constant matrix $\underline{\Phi}$ and the dynamical matrix $\underline{D}(\equiv\underline{M}^{-1/2}\underline{\Phi}\,\underline{M}^{-1/2})$ [cf. Eq. (2)], where the former can be expressed as

$$\underline{\Phi}=\underline{\Phi}^s+\underline{\Phi}^C\ , \tag{5}$$

where $\underline{\Phi}^s$ and $\underline{\Phi}^C$ correspond, respectively, to the short-range and Coulomb terms. Because of the tetrahedral (T_d) symmetry of GaAs, the off-diagonal Cartesian blocks of the short-range force-constant matrix can be shown to have the form

$$\underline{\Phi}^s(\mathrm{Ga,As})=\underline{\Phi}^s(\mathrm{As,Ga})=\begin{bmatrix}A & B & B\\ B & A & B\\ B & B & A\end{bmatrix}\ , \tag{6a}$$

$$\underline{\Phi}^s(\mathrm{Ga,Ga})=\begin{bmatrix}C_1 & D_1 & E_1\\ D_1 & C_1 & E_1\\ -E_1 & -E_1 & F_1\end{bmatrix}\ , \tag{6b}$$

and

$$\underline{\Phi}^s(\mathrm{As,As})=\begin{bmatrix}C_2 & D_2 & -E_2\\ D_2 & C_2 & -E_2\\ E_2 & E_2 & F_2\end{bmatrix}\ , \tag{6c}$$

for interactions between NN's [Eq. (6a)] and 2NN's [Eqs. (6b) and (6c)], respectively. One parameter Z (the effective charge) is used to determine $\underline{\Phi}^C$, giving a total of 11 parameters for the RIM. The evaluation of the 11 parameters involved is usually made using the neutron data of eigenfrequencies at critical points as an input with the three experimentally determined elastic constants as con-

straints. For GaAs these parameters have been determined by Kunc.[52]

In zinc-blende-type crystals, the primitive unit cell contains two atoms, which produces an eigenvalue problem of dimension 6×6 [cf. Eq. (2)]. The values of the wave vector $\mathbf{q}$ are restricted to lie within the first Brillouin zone of the fcc lattice. Hence $\mathbf{q}$ assumes the form

$$|\mathbf{q}| = \frac{\pi}{a_0}(q_1,q_2,q_3), \quad -1 \le q_1,q_2,q_3 \le 1$$

with

$$|q_1+q_2+q_3| \le \tfrac{3}{2} \, . \tag{7}$$

Here, the triples (q_1,q_2,q_3) are distributed with uniform density throughout the volume of the Brillouin zone. In terms of the frequency $\omega(\mathbf{q}j)$ and the eigenvector $e(\kappa|\mathbf{q}j)$ of the normal mode with wave vector $\mathbf{q}$ and branch index j, the elements of the Green's-function matrix [cf. Eq. (3)] can be calculated. For the most extended defect complex with three impurity atoms interacting with the NN sites, we require 33 independent elements of the Green's-function matrix for the calculation of the lattice response (see Table I).

C. Impurity perturbation

The simplest crystal defect considered here is a substitutional impurity replacing either a Ga atom ($\kappa=1$) or an As atom ($\kappa=2$) in the GaAs lattice. Both the atomic mass and the NN force constants (A,B) are assumed to be changed to (A',B') or (A'',B'') and the changes are described by the parameters

$$\epsilon_1=(M_1-M_1^I)/M_1 \, , \tag{8a}$$

$$t\equiv(A-A')/A=(B-B')/B=1-a \, , \tag{8b}$$

or

$$\epsilon_2=(M_2-M_2^I)/M_2 \tag{8c}$$

TABLE I. Green's-function matrix elements $G_{\alpha\beta}(l\kappa;l'\kappa';\omega^2-i\zeta)$ for the most extended cases of C_s/C_{2v} point-group symmetries in zinc-blende-type crystals.

Number of Green's-function matrix elements	
$g_1=G_{xx}(111;111;\omega^2-i\zeta)$	$g_{18}=G_{xx}(1\,\bar1\,\bar1;220;\omega^2-i\zeta)$
$g_2=G_{xx}(000;000;\omega^2-i\zeta)$	$g_{19}=G_{xy}(1\,\bar1\,\bar1;220;\omega^2-i\zeta)$
$g_3=G_{xx}(111;000;\omega^2-i\zeta)$	$g_{20}=G_{xz}(1\,\bar1\,\bar1;220;\omega^2-i\zeta)$
$g_4=G_{xy}(111;000;\omega^2-i\zeta)$	$g_{21}=G_{yz}(1\,\bar1\,\bar1;220;\omega^2-i\zeta)$
$g_5=G_{xx}(000;220;\omega^2-i\zeta)$	$g_{22}=G_{yy}(1\,\bar1\,\bar1;220;\omega^2-i\zeta)$
$g_6=G_{zz}(000;220;\omega^2-i\zeta)$	$g_{23}=G_{xx}(\bar1\,\bar1\,1;31\bar1;\omega^2-i\zeta)$
$g_7=G_{xy}(000;220;\omega^2-i\zeta)$	$g_{24}=G_{yy}(\bar1\,\bar1\,1;31\bar1;\omega^2-i\zeta)$
$g_8=G_{xz}(000;220;\omega^2-i\zeta)$	$g_{25}=G_{xy}(\bar1\,\bar1\,1;31\bar1;\omega^2-i\zeta)$
$g_9=G_{xx}(111;\bar1\,\bar1\,1;\omega^2-i\zeta)$	$g_{26}=G_{yx}(\bar1\,\bar1\,1;31\bar1;\omega^2-i\zeta)$
$g_{10}=G_{zz}(111;\bar1\,\bar1\,1;\omega^2-i\zeta)$	$g_{27}=G_{yz}(\bar1\,\bar1\,1;31\bar1;\omega^2-i\zeta)$
$g_{11}=G_{xy}(111;\bar1\,\bar1\,1;\omega^2-i\zeta)$	$g_{28}=G_{xx}(\bar1\,\bar1\,1;331;\omega^2-i\zeta)$
$g_{12}=G_{xz}(111;\bar1\,\bar1\,1;\omega^2-i\zeta)$	$g_{29}=G_{zz}(\bar1\,\bar1\,1;331;\omega^2-i\zeta)$
$g_{13}=G_{xx}(\bar1\,\bar1\,1;220;\omega^2-i\zeta)$	$g_{30}=G_{xy}(111;331;\omega^2-i\zeta)$
$g_{14}=G_{zz}(\bar1\,\bar1\,1;220;\omega^2-i\zeta)$	$g_{31}=G_{xz}(\bar1\,\bar1\,1;331;\omega^2-i\zeta)$
$g_{15}=G_{xy}(\bar1\,\bar1\,1;220;\omega^2-i\zeta)$	$g_{32}=G_{xx}(1\,\bar1\,\bar1;13\bar1;\omega^2-i\zeta)$
$g_{16}=G_{xz}(\bar1\,\bar1\,1;220;\omega^2-i\zeta)$	$g_{33}=G_{yy}(1\,\bar1\,\bar1;13\bar1;\omega^2-i\zeta)$
$g_{17}=G_{zx}(\bar1\,\bar1\,1;220;\omega^2-i\zeta)$	

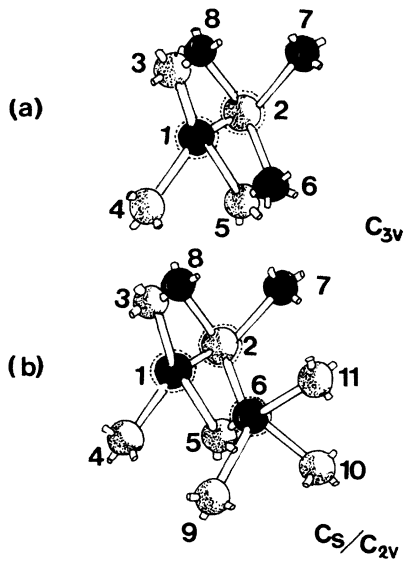

FIG. 1. Impurity models for the vibrations of one, two, and three defect centers in semiconductors: The number of atoms $1,2,\ldots,11$, and their respective coordinates, are the same as described in Ref. 46. (a) T_d case: the isolated defect $I_{\rm Ga}$ ($I_{\rm As}$) located in site 1 (2) bound to NN As (Ga) atoms at 2 (1), 3 (6), 4 (7), and 5 (8) [see Fig. 1(a)]. (b) C_{3v} case: the pair defect $I_{\rm Ga}$-$I_{2_{\rm As}}$ with the I_1 impurity occupying Ga site 1 and the I_2 impurity occupying NN As site 2 [Fig. 1(a)]. (c) The most extended case of three substitutional defects occupying sites 1, 2, and 6 as described in the text in the NN approximation [Fig. 1(b)]. If $I_1=I_6$, the impurity centers exhibit C_{2v} symmetry; otherwise, C_s.

and

$$u=(A-A'')/A=(B-B'')/B=1-b \tag{8d}$$

when the impurity M_1^I or M_2^I occupies the Ga (1) or the As (2) site, respectively [cf. Fig. 1(a)]. Before considering perturbation models to treat the vibrational properties of more complex defect centers in semiconductors, it is important to make a few comments on the choice of Eq. (8b) or (8d).

(a) For very light substitutional impurities producing the LVM's, it may be assumed that they alone vibrate in the lattice with all the host atoms "frozen" in their equilibrium sites. Under such conditions, the recoil force f_r due to short-range interactions on the substituted atom for a small displacement along one of the [100], [010], and [001] directions (the equivalent directions of the impurity vibrations in the F_2 mode) depends upon the force constants appearing on the diagonals of the coupling matrices between NN's (A) and 2NN's (F_κ and C_κ). Considering the only change to be in A ($A\to aA$), the recoil force can be written as

$$f_r=4(aA+F_\kappa+2C_\kappa) \, , \tag{9}$$

where κ ($=1,2$) denotes, respectively, the substituted atom number in the unit cell. The LVM frequency can be calculated[45] approximately by the expression $\omega_l=2\pi(f_r/M_\kappa^I)^{1/2}$, and comparison with the Green's-

function method suggest that the frequencies obtained from the empirical relation are not far off (cf. Sec. III A), which supports the assumption that vibrational energy is mainly centered on the light impurities in this LVM.

(b) It can be noted that the force constant B, a nondiagonal term of the coupling matrix between NN's is not involved in the above empirical calculation of LVM's [using Eq. (9)]. In the Green's-function method, however, our hypothesis that B varies in the same way as A (i.e., $aA=aB$) will hardly affect the calculated high-frequency impurity modes. Again, by imposing the condition $aA=aB$, the perturbation matrix $\underline{P}$ satisfies the rotational invariance requirement, which is explicitly invariant with respect to translations and crystal-symmetry operations. In other words, the change in bond-bending force constant Δf_2 (in the notation of deLaunay[53]) must be zero in the present case. To vary Δf_2 arbitrarily, on the other hand, the condition of rotational invariance should be imposed by introducing an additional parameter which has the form of a 2NN bond-bending interaction. In corroboration with the findings of earlier workers,[54] we note that the effects of rotational invariance are indeed negligible and the bond-bending force variation plays an insignificant role especially in the calculations of LVM's.[55,56]

Convinced by the above arguments, we believe that the vibrational properties of more complex defect centers can be understood in terms of simple perturbation models. To study the vibrations of a NN pair defect (C_{3v} symmetry), for example, we need a minimum of *two* (t or u) parameters, whereas for a complex defect with three impurity atoms (cf. Sec. II D), an additional parameter is required. Following Eqs. (8a)—(8d), the mass change and force-constant change parameter for an impurity to be on a Ga site (6) can be defined as [cf. Sec. II D and Fig. 1(b)]

$$\epsilon_6=(M_6-M_6^I)/M_6 \tag{10a}$$

and

$$v\equiv(A-A''')/A=(B-B''')/B=1-c\ . \tag{10b}$$

To make the perturbation models more appropriate, we have also considered direct interactions in between the impurities by two additional parameters Γ_{12} and Γ_{26}. The force variations are given by

$$F_{12}\equiv 1-ab+\Gamma_{12}=u+t-ut+\Gamma_{12} \tag{11a}$$

and

$$F_{26}\equiv 1-bc+\Gamma_{26}=u+v-uv+\Gamma_{26}\ . \tag{11b}$$

The term F_{12} (or F_{26}) <0 (or >0) corresponds to the stiffening (or softening) in the bonds 1-2 (or 2-6), respectively. Although no explicit consideration of the Coulomb interactions between the charged impurities occupying site 1, 2, or 6 has been made, their effects cause changes in the electronic charge densities (cf. Sec. III) and hence the variation of forces in the 1-2 and 2-6 bonds are contained in the F_{12} and F_{26} parameters. A complete perturbation matrix $\underline{P}$ (33×33) is formed for a special case of an impurity complex with three impurity atoms at the 1, 2, and 6 sites, respectively.

D. Group-theoretical simplifications

1. *Single substitutional defect: T_d symmetry*

Single substitutional defects in zinc-blende-type crystals retain the full point-group symmetry T_d. It is convenient to express the full-size $\underline{G}$ and $\underline{P}$ matrices (15×15) in terms of a basis of "symmetry coordinates" which transform according to the irreducible representations of the tetrahedral group. It has been shown [see Table II(a)] that the 15-dimensional irreducible representation Γ of T_d symmetry given in terms of Cartesian coordinates can be reduced to

$$\Gamma_{T_d}=A_1\oplus E\oplus F_1\oplus 3F_2\ . \tag{12}$$

The A_1 coordinate consists of a "breathing"-type motion in which the impurity atom remains stationary and the NN host atoms move radially. Again, in the F_1 and E coordinates, the impurity remains at rest while the NN atoms move. It may be seen [cf. Table II(a)] that the impurity vibrates only in the triply degenerate F_2 mode and we expect LVM's of this representation. With force-constant changes, "quasilocalized" modes can possibly occur for each type (A_1, E, F_1, F_2) of vibrations.[54,57] The forms of block diagonalization of the Green's-function and perturbation matrices belonging to each irreducible representation have already been reported and several cases of isolated point-defect vibrations are discussed elsewhere.[44–48]

2. *Nearest-neighbor pair defect: C_{3v} symmetry*

The NN pair defect is assumed to consist of an atom of mass defect $\epsilon_1=(M_1-M_1^I)/M_1$ at Ga site 1 and an atom of mass defect $\epsilon_2=(M_2-M_2^I)/M_2$ at As site 2 [cf. Fig. 1(a)]. The point-group symmetry of this defect center is C_{3v} with the axis along the bond. The vector spaces formed by the displacement of the impurity molecule and its neighbors transform according to the following irreducible representations [see Table II(b)]:

$$\Gamma_{C_{3v}}=6A_1\oplus 2A_2\oplus 8E\ . \tag{13}$$

Again in the C_{3v} symmetry, the impurity center does not move in the A_2 representation and only A_1 and E types of modes are expected to be optically active. For very light impurity atoms four LVM's are to be detected [two because of their movement along the line of joining, $\omega_1(A_1^+)\leftarrow\rightarrow$ and $\omega_4(A_1^-)\rightarrow\rightarrow$, and two as a result of movement perpendicular to it, $\omega_2(E^+)\uparrow\downarrow$ and $\omega_3(E^-)\uparrow\uparrow$, generally with $\omega_1>\omega_2>\omega_3>\omega_4$]. However, if one of the pair atoms is relatively heavier than the replaced host atom, only two vibrational modes are to be observed experimentally.[5–7] For this case, the block-diagonal $\underline{G}$ and $\underline{P}$ matrices in different irreducible representations are obtained using the symmetry coordinates of Table II(b).

3. *Impurity complexes: C_{2v} or C_s symmetry*

A more complex model with orthorhombic symmetry can be considered assuming an atom of mass defect $\epsilon_1=(M_1-M_1^I)/M_1$ at a Ga site (i.e., 1) and a second atom occupying the nearest Ga site (i.e., 6) in the [100]

TABLE II. Unnormalized symmetry coordinates for (a) a defect with T_d symmetry, (b) the NN pair defect with C_{3v} symmetry, (c) a defect center with C_s symmetry, and (d) a defect center with C_{2v} symmetry.

(a)

Atom site	A_1	$E^{(1)}$	$E^{(2)}$	$F_1^{(1)}$	$F_1^{(2)}$	$F_1^{(3)}$	$F_2^{(1)}$	$F_2^{(2)}$	$F_2^{(3)}$
1							a		
								a	
									a
2	a	a	a	a	a		b	c	c
	a	$-a$	a	$-a$		a	c	b	c
	a		$-2a$		$-a$	$-a$	c	c	b
3	$-a$	$-a$	$-a$	$-a$	a		b	c	$-c$
	$-a$	a	$-a$	a		a	c	b	$-c$
	a		$2a$		a	a	$-c$	$-c$	b
4	a	a	a	$-a$	$-a$		b	$-c$	$-c$
	$-a$	a	$-a$	$-a$		$-a$	$-c$	b	c
	$-a$		$2a$		$-a$	a	$-c$	c	b
5	$-a$	$-a$	$-a$	a	$-a$		b	$-c$	c
	a	$-a$	a	a		$-a$	$-c$	b	$-c$
	$-a$		$2a$		a	$-a$	c	$-c$	b

(b)

Atom site	A_1	A_2	$E^{(1)}$	$E^{(2)}$
1	a		a	a
	a		$-a$	a
	a			$-2a$
2	b		b	b
	b		$-b$	b
	b			$-2b$
3	c	a	$c-e$	$-c-e$
	c	$-a$	$-c+e$	$-c-e$
	d			$-2d$
4	d		d	d
	c	a	$2e$	$2c$
	c	$-a$	$c+e$	$-c+e$
5	c	$-a$	$-2e$	$2c$
	d		$-d$	d
	c	a	$-c-e$	$-c-e$
6	e	b	$f-h$	$-f-h$
	e	$-b$	$-f+h$	$-f-h$
	f			$-2g$
7	f		g	g
	e	b	$2h$	$2f$
	e	$-b$	$f+h$	$-f+h$
8	e	$-b$	$-2h$	$2f$
	f		$-g$	g
	e	b	$-f-h$	$-f+h$

direction with mass defect $\epsilon_6=(M_6-M_6^I)/M_6$. The point-group symmetry is C_{2v} if $\epsilon_1=\epsilon_6$; otherwise it is C_s. If the force-constant changes are confined in the NN approximation, the size of the defect space will increase to 33×33 and the vector spaces formed by the displacements of the impurity molecule and its neighbors may transform according to the following irreducible representations [see Tables II(c) and II(d)]:

$$\Gamma_{C_{2v}}=10A_1\oplus6A_2\oplus8B_1\oplus9B_2 \tag{14a}$$

and

TABLE II. (*Continued*).

(c)			(d)				
Atom site	A_1	A_2	Atom site	A_1	A_2	B_1	B_2
1	a	a	1	a	a	a	a
	a	$-a$		a	$-a$	$-a$	a
	b			b			b
2	c	b	2			b	c
	c	$-b$				$-b$	c
	d			c			
3	e	c	3	d	b	c	d
	e	$-c$		d	$-b$	$-c$	d
	f			e			e
4	g	d	4	f	c	d	f
	h	e		g	d	e	g
	i	f		h	e	f	h
5	h	$-e$	5	g	$-d$	$-e$	g
	g	$-d$		f	$-c$	$-d$	f
	i	$-f$		h	$-e$	$-f$	h
6	j	g	6	$-a$	$-a$	a	a
	j	$-g$		$-a$	a	$-a$	a
	k			b			$-b$
7	l	h	7	i	f	g	i
	m	i		$-i$	f	$-g$	i
	n	j		j		h	
8	m	$-i$	8	$-i$	$-f$	g	i
	l	$-h$		i	$-f$	$-g$	i
	n	$-j$		j		$-h$	
9	o	k	9	$-g$	d	$-e$	g
	p	l		$-f$	c	$-d$	f
	q	m		h	$-e$	f	$-h$
10	p	$-l$	10	$-f$	$-c$	d	f
	o	$-k$		$-g$	$-d$	e	g
	q	$-m$		h	e	f	$-h$
11	r	n	11	$-d$	$-b$	c	d
	r	$-n$		$-d$	b	$-c$	d
	s			e			$-e$

$$\Gamma_{C_s} = 19A_1 \oplus 14A_2 \ . \tag{14b}$$

The impurity complex with C_{2v} point-group symmetry can give rise to A_1, B_1, and B_2 types of vibrations, whereas in the C_s-symmetry case both A_1 and A_2 types of modes will be optically allowed. Since the degeneracies are lifted, *six* impurity bands are expected in each case of the impurity centers with light defect atoms. A special case of C_s symmetry with a vacancy at site 6 (say) and impurity at site 1 will lift the degeneracy of the impurity oscillator at site 1 and one thus obtains three nondegenerate modes. Again the block-diagonal $\underline{G}$ and $\underline{P}$ matrices in each of the irreducible representations of point groups C_{2v} and C_s are obtained using the appropriate symmetry coordinates given in Tables II(c) and II(d).

III. NUMERICAL COMPUTATIONS AND RESULTS

We have computed the bulk Green's-function matrix $\underline{G}$ by incorporating phonons (eigenvectors and eigenvalues) obtained from RIM11.[51] The hypotheses adopted in defining the perturbation matrix (cf. Sec. II) are those of Refs. 44–47. The first case with *one* substitutional defect involves five atoms with T_d symmetry. The solutions of Eq. (1) belonging to A_1, E, F_1, and F_2 irreducible representations were carried out with t (or u) varying between $+1$ and -1 (see Figs. 2 and 3) for cases when the defect occupies the Ga and the As site, respectively. In most cases with very light impurities Eq. (1) gives only solutions corresponding to vibrational modes of F_2 symmetry.

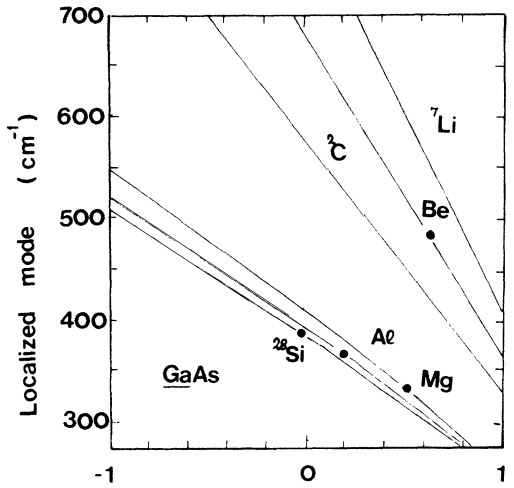

FIG. 2. Calculated frequencies of the LVM's in the F_2 irreducible representation for various isolated defects occupying Ga sites in *Ga*As as a function of the force-constant–change parameter t; ● represents the experimental data.

In Table III we have compiled the experimental data of LVM's along with the t (or u) values for which the solutions of Eq. (1) in the F_2 representation occur in III-V and II-VI compounds. This we believe will serve as a good starting point to analyze the existing ir data of LVM's for complex defect centers and also help obtain a set of best-fit parameters which are physically realistic. We consider the following cases.

A. Single substitutional defects

From the existing experimental studies in GaAs, there is considerable evidence that silicon behaves like an amphoteric defect: donor behavior when substitutional on the Ga sublattice and acceptor behavior when it occupies the As sublattice. In each case the point-group symmetry is T_d and the ir spectroscopy provides triply degenerate LVM frequency near ~ 399 cm^{-1} for $^{28}Si_{As}$ and near

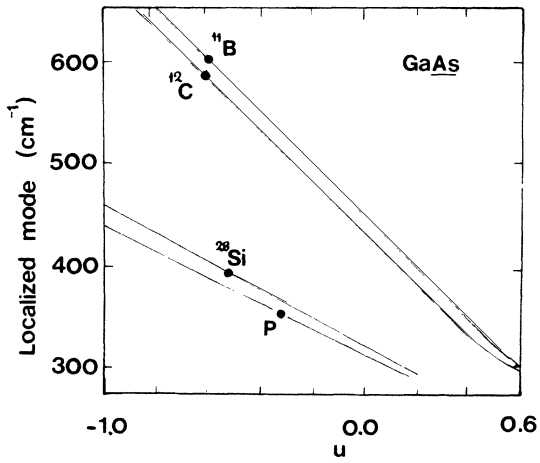

FIG. 3. Same key as Fig. 2, but for defects occupying As sites in Ga*As* as a function of force-constant–change parameter u.

TABLE III. Comparison of the calculated LVM's due to several isoelectronic (i), donor (d^+), and acceptor (a^-) isolated defects of comparable masses in various III-V and II-VI compound semiconductors.

System	LVM's (cm)$^{-1}$ Expt.[a]	Calc. in MDA	t or u[b] relative change in force constant
*Ga*As:Al (i)	361.6[c]	389.42	0.18
*Ga*As:^{24}Mg (a^-)	331.2[c]	411.01	0.50
*Ga*As:^{25}Mg (a^-)	326.2[c]	403.37	0.50
*Ga*As:^{26}Mg (a^-)	321.7[c]	396.20	0.50
*Ga*As:^{28}Si (d^+)	384.0	382.51	−0.03
*Ga*As:^{9}Be (a^-)	482.0	659.04	0.63
*Ga*As:^{10}B (i)	540.2	624.07	0.33
*Ga*As:^{6}Li (a^-)	482.31	850.10	0.89
*Ga*As:^{7}Li (a^-)	449.61	816.07	0.89
Ga*As*:P (i)	354.8[c]	314.51	−0.31
Ga*As*:^{28}Si (a^-)	398.61	324.02	−0.54
Ga*As*:^{12}C (a^-)	582.4	443.10	−0.61
Ga*As*:^{11}B (a^-)	601.4	457.61	−0.607
*Ga*P:^{27}Al (i)	444.7	484.71	0.23
*Ga*P:^{28}Si (d^+)	464.9	478.11	0.08
Ga*P*:^{12}C (a^-)	606.2	515.05	−0.374
Ga*P*:^{14}N (i)	496.0	485.03	−0.03
Ga*P*:O (d^+)	~199.0	461.54	~0.90
Ga*P*:^{11}B (a^-)	624.5	531.02	−0.37
*Zn*Se:^{6}Li (a^-)	412.0	695.03	0.97
*Zn*Se:Be (i)	450	553.05	0.51
*Zn*Se:^{26}Mg (i)	334	333.35	−0.05
*Zn*Se:Al (d^+)	358.91	327.80	−0.30
*Zn*Te:^{26}Mg (i)	260.5	253.26	−0.10
*Zn*Te:Al (d^+)	313	245.90	−0.51
*Zn*S:^{25}Mg (i)	377.5	358.90	−0.20
*Zn*S:Al (d^+)	438	356.81	−0.76
*Cd*Te:^{25}Mg (i)	245.0	286.11	0.36
*Cd*Te:Al (d^+)	299.0	275.91	−0.23

[a]References 5–7.
[b]This work.
[c]High-resolution measurements (our data).

~ 384 cm^{-1} for $^{28}Si_{Ga}$ in GaAs. Isotopically shifted peaks have also been detected due to $^{29}Si_{Ga}$ and $^{30}Si_{Ga}$ (cf. Table III). In the mass-defect approximation (MDA) (neglecting changes in force constants, i.e., $t=0$ or $u=0$), our calculations of the LVM due to a Si donor or acceptor provide values smaller than the experimental ones. This requires stiffening in the NN impurity-host bonding to bring the local-mode frequencies into agreement with the existing data. Table III also reflects a large variation of t or u parameters, when we pass from isoelectronic (i) to charged [donor (d^+) or acceptor (a^-)] defect substitution of comparable masses in various semiconductors. A comparison with the existing experimental data shows clearly that there exists no correlation with the signs of t or u and the size of the impurity-host atoms. After analyzing more than *eighty* cases of LVM's due to substitutional defects in *fifteen* semiconductors, we, however, find the following behavior for closest mass a^-, i, and

d^+ occupying III, (II) and V (VI) sites in III-V (II-VI) compounds:

$$\Delta t\{a^-_{\mathrm{III\,(II)}} - i_{\mathrm{III\,(II)}}\} > 0, \quad \text{softening} \tag{15a}$$

$$\Delta t\{d^+_{\mathrm{III\,(II)}} - i_{\mathrm{III\,(II)}}\} < 0, \quad \text{stiffening} \tag{15b}$$

$$\Delta u\{a^-_{\mathrm{V\,(VI)}} - i_{\mathrm{V\,(VI)}}\} < 0, \quad \text{stiffening} \tag{15c}$$

and

$$\Delta u\{d^+_{\mathrm{V\,(VI)}} - i_{\mathrm{V\,(VI)}}\} > 0, \quad \text{softening} . \tag{15d}$$

Again, these trends are found independent of the long-range Coulomb forces and we strongly argue that the charged impurities in semiconductors affect only the short-range forces *via* redistribution of the electron charge density.[58–60] To further stress this point, let us examine the bonding mechanism in unperturbed host lattices. For compounds from the same row, Ge-GaAs-ZnSe (or Sn-InSb-CdTe), the covalent bonding is apparent in Ge, where the charge is centered midway between the two atoms. For *partially covalent* GaAs, the bonding charge is displaced towards the As atom and, in *partially ionic* ZnSe, nearly all the charge is centered near the Se atom [cf. Fig. 4(a)]. If ^{27}Al (i) is substituted for Ga in GaAs, the Al—As bond is represented by a cloud of valence electrons located near the As region. Replacing ^{27}Al by an acceptor ^{24}Mg (a^-) will cause the electrostatic forces to shift the electron cloud towards the As core, the bond becomes more ionic, and we observe its softening. On the contrary, if Al is replaced by a donor ^{28}Si (d^+), its additional positive charge will attract the electron cloud, increasing the covalency of the bond and consequently we observe its stiffening (see Table III). It can be noted that for a^-, i, and d^+ defects occupying the V (VI) site in III-V (II-VI) compounds, the shift in the electronic charge density and thus the change in the covalency of the bond occurs in just the opposite way—a result in complete corroboration with our calculated trends of force variations [cf. Fig. (4b) and Table III]. To the best of our knowledge, the only work where the electronic charge-density contours are obtained both for the perfect and imperfect systems is the recent calculations by Baraff *et al.*[61] The authors of Ref. 61 have clearly shown the shift of electron charge density towards the O donor in Ga*P*, causing softening in the Ga—O bond [cf. Fig. 4(c)], in full agreement with our observations. The present simple physical understanding of the bonding situation in terms of the general magnitude of the "impurity-host parameters" (t or u) will hopefully provide us with the most productive means of establishing and identifying the *microstructure* features of the defects and their relationship to the optical experiments.

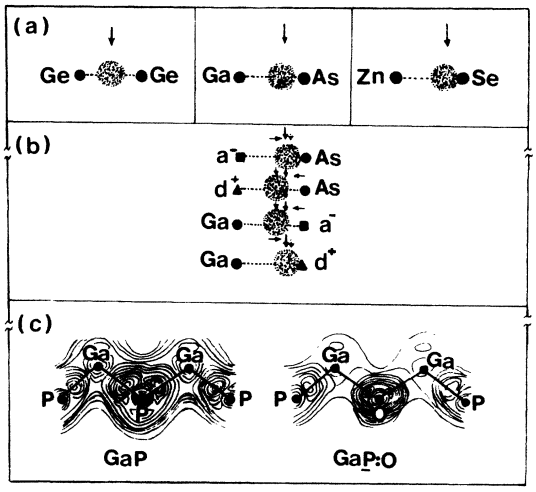

FIG. 4. Force-variation correlation with bond ionicity (covalency) in semiconductors: (a) perfect systems (Ref. 59). (b) Imperfect systems (our observation). (c) Calculated electronic charge-density contours for GaP and Ga*P*:O (Ref. 61).

B. Ga isotopic fine structure of LVM's due to B antisite defects in GaAs

Van Vechten[62] was the first to predict theoretically the existence of both self- (As_{Ga}, Ga_{As}) and foreign (B_{As}) antisite defects in GaAs. Using EPR measurements on samples grown from As-rich or stochiometric melts, Wagner *et al.*[8] have provided support for the As_{Ga} centers. Now, there is a general consensus that As-rich GaAs materials are electrically compensated by negatively charged C_{As} acceptors and by positively charged deep donors (As_{Ga}). In recent years,[16,30,63] a great deal of effort has been made in seeking experimental evidence for the Ga antisite defects and to examine the role of B impurities.

Detailed ir measurements and its analyses have led Woodhead *et al.*[34] to argue that in addition to isoelectronic B_{Ga} defect lines (540 and 517 cm^{-1}) in GaAs, the LVM's detected earlier (at 628 and 601 cm^{-1}) due to B(2) centers actually arise from defects with antisite $^{10}B_{As}$ ($^{11}B_{As}$) structure. Another experiment that supported the analyses and provided direct evidence for the B_{As} centers is the work of Gledhill *et al.*,[14] where the 601-cm^{-1} (628-cm^{-1}) transition has been resolved by FTIR into four or possibly five fine-structure lines. Comparison with similar measurements by Theis *et al.*[15] for $^{28}Si_{As}$ and $^{12}C_{As}$ in GaAs concluded that the line at $\sim$601 cm^{-1} originates from $^{11}B_{As}$ and the fine structure arises from the Ga isotopic masses in different NN configurations. Again, the relative band strengths of the lines are directly proportional to the natural abundance of the Ga isotopes involved in various arrangements (see Table IV).

Considering an isolated impurity I (say B) on the As site, I_{As}, there occur *five* isotopic combinations on the four NN sites. From group-theoretic arguments, it can be shown that there are *nine* lines—all allowed by the ir selection rules (see Table IV). The probability of LVM strength appearing in each line of different configurations is also given in Table IV. The Green's-function theory developed in the preceding section is applied to understand the observed Ga isotopic fine structure in the Ga*As*:^{11}B system. The shifts in the LVM's due to Ga isotopic masses in Ga*As*:^{11}B are calculated considering appropriate symmetry properties for each of the arrangements confined to *five* atoms and using *one* perturbation parameter value $u = -0.607$ (Table III). The results are displayed in Fig. 5 and compared with the experimental data of Gledhill *et al.*[14] Despite the simplicity of the per-

TABLE IV. Ga isotopic masses involved in different NN configurations of the GaAs:^{11}B system. Considering the abundance of the ^{69}Ga as 60.4 at. %, the probability of the LVM's appearing in each configuration is also given.

System[a]	Symmetry[a]	Mode[a]	Probability factor for each of the LVM lines with $C=0.604$	
$^{69}Ga_4$-$^{11}B_{As}$	T_d	F_2	C^4	0.133
$^{69}Ga_3$-$^{11}B_{As}$-$^{71}Ga_1$	C_{3v}	A_1,E	$\frac{4}{3}C^3(1-C)$, $\frac{8}{3}C^3(1-C)$	0.116, 0.233
$^{69}Ga_2$-$^{11}B_{As}$-$^{71}Ga_2$	C_{2v}	A_1,B_1,B_2	$2C^2(1-C)^2$, $2C^2(1-C)^2$, $2C^2(1-C)^2$	0.114, 0.114, 0.114
$^{69}Ga_1$-$^{11}B_{As}$-$^{71}Ga_3$	C_{3v}	A_1,E	$\frac{4}{3}C(1-C)^3$, $\frac{8}{3}C(1-C)^3$	0.05, 0.10
$^{71}Ga_1$-$^{11}B_{As_1}$	T_d	F_2	$(1-C)^4$	0.0246

[a]See the text and Fig. 6.

turbation models, the magnitude and the strength of the calculated isotopic shift of *nine* lines coalescing to *five* bands is in good qualitative accord with the FTIR data.

C. "d^+-a^-" silicon pairs in GaAs

The NN "d^+-a^-" silicon pairs in GaAs exhibit C_{3v} symmetry and *four* LVM's are expected, *two* being longitudinal and nondegenerate and *two* transverse and doubly degenerate. The displacement of the pair atoms is *symmetric* in one longitudinal and one transverse mode (A_1^+,E^+) and is *antisymmetric* in the other two (A_1^-,E^-). Earlier ir measurements have identified *two* symmetric modes near 464 cm^{-1} (A_1^+) and 393 cm^{-1} (E^+), while it is speculated that the bands observed near 367 and 369 cm^{-1} belong to *two* other unidentified but Si-related defects which shall be considered later in this section. Although antisymmetric modes were not observed, it was, however, erroneously thought[29,27] at one time that the line near 367 cm^{-1} was another Si-pair mode.

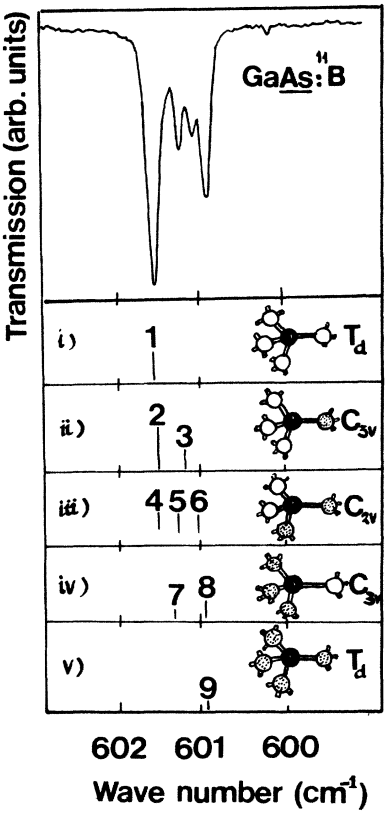

FIG. 5. Isotopic fine structure of LVM's in GaAs:^{11}B observed under high-resolution FTIR spectroscopy (Ref. 16). Calculated results [panels (i)–(v)] of LVM's based on the Green's-function theory with models of Table IV. In the lower panels the numbers 1,2,3, . . . ,9 represent the position and the relative heights of the lines according to their probability of occurrence (see Table IV): ○, ^{69}Ga; ◎, ^{71}Ga; ●, ^{11}B.

In Fig. 6 we have displayed the results of our calculations for the LVM's in the MDA for $^{28}Si_{Ga}$ paired with other impurities on the As site in GaAs. It clearly shows the possibility of the occurrence of four [$\omega_1(A_1^+)$, $\omega_2(E^+)$, $\omega_3(E^-)$, and $\omega_4(A_1^-)$] LVM's, if the impurity masses are much smaller than the host lattice atoms (e.g., $^{28}Si_{Ga}$-$^{11}B_{As}$, etc.). However, if one of the pair atoms is heavier, the antisymmetric modes will fall into the band continuum and only two modes are expected. At $\epsilon_2=0$, $\omega_1(A_1^+)=\omega_2(E^+)$, which provides the LVM frequency of the isolated case ($^{28}Si_{Ga}$) in GaAs. The effect of F_{12} on the LVM's is also shown in Fig. 6. As expected, it mainly affects the impurity modes related with the movement of

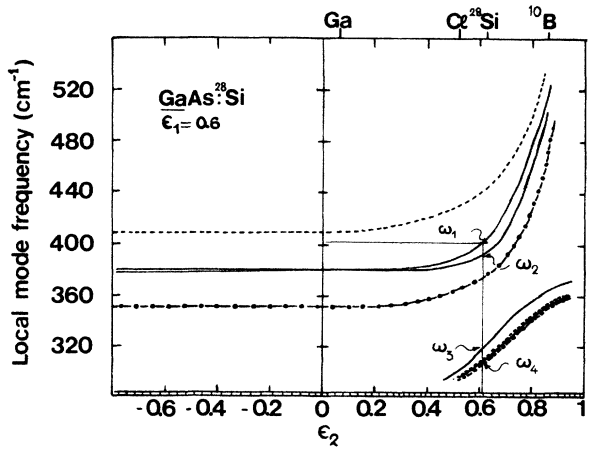

FIG. 6. Calculated LVM's due to ^{28}Si occupying Ga sites and paired with other impurities occupying As sites in GaAs. (a) MDA (——), (b) $F_{12}=-0.24$ (— — —), and (c) $F_{12}=+0.4$ (—·—·—·), $t=u=F_{12}=0$.

atoms along their line of joining, while the modes related with the movement of atoms perpendicular to it remain almost unchanged. All the vibrational modes are, however, affected with the variation of impurity-host parameters (t and u).

Perusal of Fig. 6 reveals that there should occur four LVM frequencies in the MDA for a ^{28}Si-pair defect in GaAs. Because of the very high frequency of the observed LVM at 464 cm^{-1}, it seems clear that this corresponds to the A_1^+ mode and it is inferred that the force constant associated with the bond-connected Si pair is stronger than the bonds from the Si to the Ga or As neighbors. Using the same values of force variations for the isolated cases of Si defects (cf. Table III), one may obtain $F_{12}=-0.59$, and with this stiffening in the Si-pair bond we are able to reproduce the A_1^+ and E^+ modes in excellent agreement with the observed ones. Again, the same value of F_{12} provides results for the shift of the A_1^+ mode for $^{28}Si_{Ga}$-$^{30}Si_{As}$, $^{30}Si_{Ga}$-$^{28}Si_{As}$, and $^{30}Si_{Ga}$-$^{30}Si_{As}$ pairs at 455.2, 457.3, and 448.7 cm^{-1}, in good accord with the recent high-resolution measurements of Theis and Spitzer,[30] which reported the values 455.8, 457.01, and 448.7 cm^{-1}, respectively. With the present choice of perturbation model, our calculations predict the E^- mode near 323 cm^{-1} and an A_1^- mode close to the maximum phonon frequency of GaAs.

Let us now return to the absorption bands (at 367 and 369 cm^{-1}) which are believed to originate from separate centers, each involving one silicon and a native (vacancy or antisite) defect. Although there are no definitive interpretations for these modes, the earlier ir data (low resolution) showed that the FWHM for the 367-cm^{-1} band is significantly smaller ($\sim$1.5 cm^{-1}) than that of 2 cm^{-1} for the 369-cm^{-1} line. By correlating the absorption strengths of these lines to precompensation values of carrier densities, the 367-cm^{-1} line was best-fitted by assuming it to be a donor, whereas the 369-cm^{-1} line was fitted by assuming it to be an acceptor, although this evidence is felt to be statistically inconclusive.[30] Recent high-resolution FTIR measurements of Theis and Spitzer[30] find no splitting in the former (367 cm^{-1}, A band) line, which retained a width of about $\sim$1 cm^{-1}, while the latter band is split into three resolved components (368.31 cm^{-1}, B line; 369.53 cm^{-1}, C line; and 370.7 cm^{-1}, D line). From a variety of evidence, including the large FWHM of the A band near 367 cm^{-1}, it was concluded that the Si_{As}-As_{Ga} defect was the most probable, as this would create an (unresolved) broadening of the A line due to combinations of the three NN Ga isotopes to such a center and, furthermore, would have a donor behavior. Newman[64] has, however, claimed very recently that he has resolved the 367-cm^{-1} band into a doublet which is compatible with its identity being Si_{Ga}-Ga_{As} with two isotopes of Ga creating the two features in the doublet. Contrary to the observed electrical nature, such a pair would have a net acceptor behavior. Finally, very little has been speculated about the identity of the B-C lines (the former Si-Y center at 369 cm^{-1}), except that since they occur only in electron-irradiated or Cu-compensated silicon-doped samples, involvement of native vacancies is possible. (The 367-cm^{-1} LVM appears in all samples, regardless of compensation method.)

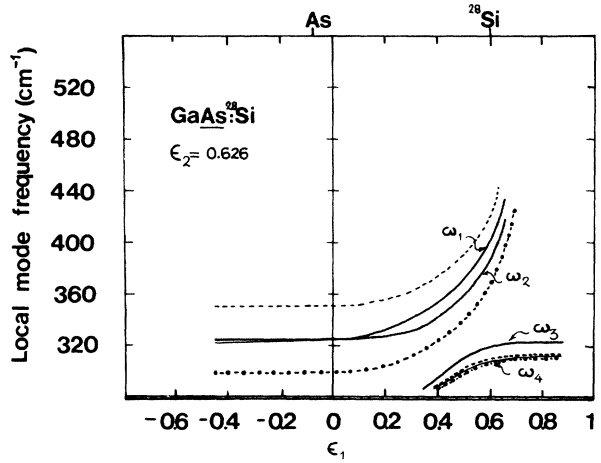

FIG. 7. Same key as of Fig. 4, but for ^{28}Si occupying As sites and paired with other impurities occupying Ga sites in GaAs. (a) MDA (——), (b) $F_{12}=-0.3$ (— — —), and (c) $F_{12}=0.3$ (—·—·—·), $t=u=F_{12}=0$.

Using the Green's-function theory (cf. Sec. II), we have evaluated the possibilities of the occurrence of impurity centers with *antisite* defects, proposed to be responsible for the 367- and 369-cm^{-1} bands. In the MDA our results for the impurity center $^{28}Si_{Ga}$-$^{69}Ga_{As}$ provide *two* nearly identical frequencies ($A_1=E$ at $\simeq$383 cm^{-1}) (cf. Fig. 6). The A_1 mode shifts on the high-frequency side with *stiffening* in the "pair bond" (i.e., with $F_{12}<0$), while with *softening* (i.e., $F_{12}>0$) it lowers with respect to the E mode which remains almost unchanged. With $F_{12}=0.13$, a softening in the "pair bonding," the A_1^+ mode matches exactly to the 367-cm^{-1} band while the E^+ line remains close to the 383-cm^{-1} frequency (the LVM frequency for the isolated $^{28}Si_{Ga}$ in GaAs). Changing $^{69}Ga\rightarrow{}^{71}Ga$ in the above pair defect lowers the A_1 mode frequency by 0.12 cm^{-1}, supporting the observation of a doublet for the 367-cm^{-1} LVM. Similar to Fig. 6, the impurity modes due to $^{28}Si_{As}$ paired with other defects on the NN Ga site are also displayed in the MDA (see Fig. 7). Assuming a self-antisite-defect As_{Ga} in the pair

TABLE V. Ga isotopic fine structure of LVM's (bands B,C,D) observed (see text) in the high-resolution FTIR measurements (probably) due to the $^{28}Si_{As}$-As_{Ga} pair defect in GaAs.

Defect center	LVM's (cm^{-1}) Expt.[a]	Calc.[b]
$^{69}Ga_3$-$^{28}Si_{As}$-As_{Ga}	D: 370.7	370.3
$^{69}Ga_2$-$^{28}Si_{As}$-As_{Ga} + $^{71}Ga_1$	C: 369.53	370.12, 369.91
$^{71}Ga_2$-$^{28}Si_{As}$-As_{Ga} + $^{69}Ga_1$		369.69, 369.50
$^{71}Ga_3$-$^{28}Si_{As}$-As_{Ga}	B: 368.31	368.94

[a]Reference 30.
[b]See text for details of this impurity model.

$^{28}Si_{As}$-As_{Ga} will leave four possibilities of random population of three NN Ga sites to $^{28}Si_{As}$ by the two Ga isotopes corresponding to $^{69}Ga_3$, $^{69}Ga_2+^{71}Ga_1$, $^{69}Ga_1+^{71}Ga_2$, and $^{71}Ga_3$. For the defect ($^{69}Ga_3$-$^{28}Si_{As}$-As_{Ga}), our calculations in the MDA provide two modes with nearly identical values ($A_1^+=E^+$ at 323 cm^{-1}). The A_1^+-mode frequency shifts to the higher value with stiffening in the pair bonding, leaving the E^+ mode nearly unchanged at 323 cm^{-1}. With $F_{12}=-0.56$, our results for the Ga isotopic effect in the above pair-defect vibrations are reported in Table V and compared with the ir (high resolution) data of Theis and Spitzer[30] for the 369-cm^{-1} features.

D. "Si-Li" pairs in GaAs

When Li is used to compensate Si-doped GaAs, LVM's due to "Si-Li" pairs have been observed.[30] The Si and Li atoms are assumed to be on the second-neighbor Ga sites and the pair defect has a C_s symmetry. Six LVM's are observed by ir spectroscopy and are attributed to *three* (405, 379, and 374 cm^{-1}) predominantly ^{28}Si modes and *three* (455, 448, and 438 cm^{-1}) ^7Li modes, as determined by the isotopic frequency shifts when $^7Li\rightarrow{}^6Li$ and $^{28}Si\rightarrow{}^{30}Si$. It should be noted that the Li modes in the "Si-Li" pair are at higher frequencies than the Si modes, but not as high as one would predict in the MDA (see Fig. 2). With a perturbation relationship $\bar{\nu}^2=\frac{1}{3}\sum_{i=1}^{3}\nu_i^2$, one can approximately calculate the perturbed frequency $\bar{\nu}$ of a defect in terms of its split frequencies ν_i, and this provides values at 385.51 and 446.49 cm^{-1}, respectively, for $^{28}Si_{Ga}$ and $^7Li_{Ga}$ in GaAs to be compared with the experimental data at 383.68 and 449.64 cm^{-1}.

From Fig. 2 we have estimated the NN force-constant–change parameter ($t=0.89$) for *Ga*As:^{7}Li, and with this value it is found that the LVM frequency shifts to 482 cm^{-1} for $^6Li_{Ga}$, in close agreement with the experimental results of Theis and Spitzer[30] of 482.13 cm^{-1}. To describe the vibrations of Si-Li pairs in GaAs, we find that only *three* (t,u,v) out of *five* parameters are necessary to provide the best fit to the observed LVM's (see Table VI). Included in this table are experimental values for other isotopic combinations in addition to the previously reported ($^7Li_{Ga}$-$^{28}Si_{Ga}$) LVM's.

TABLE VI. Localized vibrational modes due to Li-Si pair defects of C_s symmetry in GaAs at 80 K. The results of the Green's-function theory (see text) are also given for comparison.

System	LVM's (cm^{-1}) Expt.	Calc.[d]	Mode
$^7Li_{Ga}$-$^{28}Si_{Ga}$[a]	454.19	453.20	A_1
	447.39	449.61	A_1
	437.75	441.50	A_2
	404.84	405.01	A_1
	378.19	379.63	A_2
	372.72	372.10	A_1
$^7Li_{Ga}$-$^{30}Si_{Ga}$	454.19	453.17	A_1
	~447.0[b]	449.43	A_2
	437.73	441.48	A_2
	391.67	392.31	A_1
	369.56	371.03	A_2
	364.37	365.13	A_1
$^6Li_{Ga}$-$^{28}Si_{Ga}$	487.11	484.13	A_1
	479.88	480.01	A_1
	469.47	474.81	A_2
	404.88	405.70	A_1
	378.23	379.81	A_2
	~374.0[c]	374.0	A_1
$^6Li_{Ga}$-$^{30}Si_{Ga}$	487.11	484.07	A_1
	479.88	479.96	A_1
	469.47	474.70	A_2
	393.79	392.82	A_1
	367.92	371.30	A_2
	362.47	365.20	A_1

[a]Reference 30.

[b]Interference from $^{30}Si_{Ga}$-$^{30}Si_{As}$ makes exact determination impossible.

[c]Interference from $^{30}Si_{Ga}$ line.

[d]See text for details of this pair-defect model. The parameters fitted were $t=0.91$, $u=-0.70$, and $v=0.11$. Alternately, this can be expressed as $t=0.91$, $F_{12}=0.847$, $F_{26}=-0.513$, and $v=0.11$.

IV. DISCUSSION AND CONCLUSIONS

In contrast to the earlier findings of Gaur *et al.*,[65] we have noted that the relative variations of NN forces are large even for isoelectronic defects and quite appreciable for charged defects in compound semiconductors. Bellomonte[66] has suggested a possible size effect for the large softening in *Ga*As:B, as the covalent radius of B (0.88 Å) is much smaller than the replaced Ga (1.26 Å) atom. Although we do find appreciable softening for B in GaP and GaAs, stiffening is indicated for B in InP. Further evidence that the size of substitutional atoms does not dominate bond strength can be found for N and C in III-V compounds, both of which have radii smaller than B. We, on the other hand, propose empirical relationships [Eqs. (15a)–(15d)] which provide correction to the force constants for closest mass isoelectronic defects and impurities carrying static charges. Typically, the absolute values of the relative variations of Δt and Δu for single charge (a^-,d^+) and isoelectronic (i) defects producing LVM's in all the II-VI and III-V compounds are found to lie well within 15–35%. On the other hand, for double charge (a^{2-}, e.g., Li) and isoelectronic (i, e.g., B) defects, we find that the value of the force variation Δt is approximately twice as large as for the single-charge Be^- and isoelectronic B occupying Ga site in GaAs (cf. Table III).

From Eqs. (15a)–(15d), it can be noted that there is a net correlation between the force perturbation and modification of the bond ionicity (or covalency). It is already shown qualitatively that the increase or decrease of the force variation due to charged impurities varies in the same sense as does the increase or decrease of the covalency of the bond. The impact of the increasing or decreasing bond ionicity on the interatomic forces may be determined from its comparison with the short-range coupling between first neighbors (parameters A and B) as obtained from the lattice dynamics. In Fig. 8 we have plotted A against the interatomic distance r_0 for various elemental

and compound semiconductors. Similar behavior is noticed if B versus r_0 is plotted. From Fig. 8 it is apparent that the two parameters are important for characterization of the coupling: bond ionicity and bond length. It can be noted that (a) in groups II-VI, III-V, and IV-IV the coupling decreases slowly with increasing bond length, and (b) for compounds in the same row, e.g., Ge-GaAs-ZnSe-CuBr, the bond length is practically constant but the coupling A decreases slowly with increasing ionicity or decreasing covalency. This behavior provides added support to the fact that the increase or decrease of force perturbation due to charged impurities varies in the same way as the increase or decrease of the covalency of the bond.

In Fig. 5 the calculated splitting pattern of LVM's in Ga*As*:^{11}B is compared with the FTIR measurements of Gledhill *et al.*[14] Despite the simplicity of the perturbation models, the magnitude and the strength of the calculated isotopic shifts of *nine* lines coalescing to five bands are in good qualitative accord with the ir data. This not only shows the reliability of the Green's-function method, but also demonstrates its superiority over the perturbation[37] and the cluster-Bethe—type calculations[38] where additional force-variation constraints are used (sometimes with no physical meaning) to match the observed isotopic shifts. Although Woodhead *et al.*[34] have provided convincing evidence that the LVM frequency at 601 cm^{-1} (628 cm^{-1}) originates from the $^{11}B_{As}$ ($^{10}B_{As}$) antisite defect in its single negative charge state, the B_{As} defect, however, can have B_{As}^{-2} or B_{As}^{0} states, depending upon the position of the Fermi level. As pointed out earlier for single charge (a^-) and isoelectronic (i) defects in Ga*As*, the relative variation of Δu should be of the order of ~ -0.3. Table III indicates that this is indeed the case for $^{11}B_{As}$, $^{12}C_{As}$ (acceptors), and P_{As} (isoelectronic) impurities. Again, it has been found that the LVM's for $^{10}B_{As}$, $^{11}B_{As}$, $^{12}C_{As}$, and $^{13}C_{As}$ form an almost linear sequence with the mass-defect parameter. The implication of all this is that the impurities in the *two* centers (B_{As} and C_{As}) are present in the same charge state, providing added support to the arguments by Woodhead *et al.*[34] From our analyses of force variations due to charged defects, we expect LVM's to occur at $\sim$663 and $\sim$533 cm^{-1} for $^{11}B_{As}^{2-}$ and $^{11}B_{As}^{0}$, respectively. Because of the low background absorption, the mode of $^{11}B_{As}^{2-}$ (should it exist) should be detectable, while the line due to $^{11}B_{As}^{0}$ would be obscured due to its probable occurrence in the region of high lattice absorption.

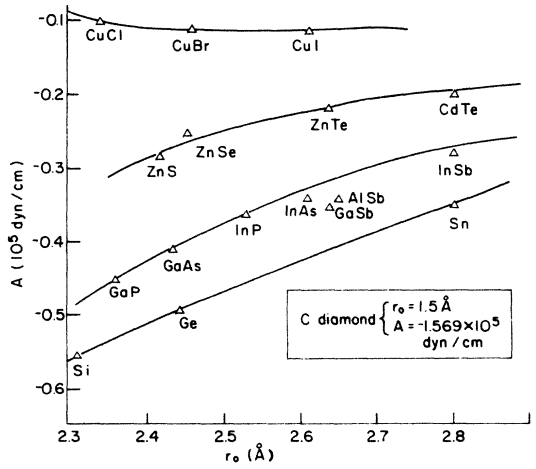

FIG. 8. Variation of the NN force constant A of RIM11 versus interatomic separation r_0 for various I-VII, II-VI, III-V and IV-IV crystals.

From the ir measurements in Si-doped GaAs, it is apparent that the linewidths and peak frequencies of the bands at $\sim$464 and 393 cm^{-1} are not influenced by any charge compensation, suggesting that the modes are related with the NN "d^+-a^-" Si-pair vibrations. Our calculations have suggested that the band near $\sim$464 cm^{-1} is a singly degenerate axial stretching mode with A_1^+ symmetry and the one at $\sim$393 cm^{-1} is the doubly degenerate mode with E^+ symmetry. As stated earlier, the lines near $\sim$367 and 369 cm^{-1} do not correlate in strength to the known pair absorption bands at 393 and 464 cm^{-1}, respectively, and therefore cannot be related to the Si pairs. From the analyses of recent high-resolution ir data, it is believed that the modes at 367 and 369 cm^{-1} are originating from separate centers, each involving one silicon and a native defect presumably $^{28}Si_{Ga}$-Ga_{As}, $^{28}Si_{As}$-As_{Ga}, or Si vacancy center. With $F_{12}=0.13$, a softening in the "pair bonding" in the defect center $^{28}Si_{Ga}$-$^{69}Ga_{As}$, our Green's-function calculations provide an A_1^+ mode at 367 cm^{-1} in close agreement with the ir data and give the E^+ line (at 383 cm^{-1}) near the LVM frequency of the isolated $^{28}Si_{Ga}$ in GaAs. Changing $^{69}Ga \rightarrow {}^{71}Ga$ lowers the A_1-mode frequency by $\sim$0.12 cm^{-1}, which provides for a doublet when the 367-cm^{-1} band is completely resolved. If the defect center $^{28}Si_{As}$-As_{Ga} is considered responsible for the 369-cm^{-1} band, there will be four possibilities of random population of *three* NN Ga sites to $^{28}Si_{As}$ by the *two* Ga isotopes which will provide shift in the A_1^+ band (see Table V). With $F_{12}=-0.56$, the Ga isotopic shift in the A_1^+ modes are in good agreement with several of the features of the resolved 369-cm^{-1} band.[30] We further predict the possibility of another band (E^+ line) to be detected near $\sim$323 cm^{-1}. Except in a unique Li-diffused sample where a line does appear near 328 cm^{-1}, the measurements performed by Theis and Spitzer[30] on the other *thirteen* samples have failed to reveal any related structure near this frequency region. Although the simple models proposed here to understand the origin of 367- and 369-cm^{-1} bands do explain most of the features observed in the high-resolution FTIR measurements, there still remain, however, some questions to be answered. One obvious problem is the electrical character: Correlations of absorption strengths after compensation to precompensation carrier densities have indicated donor behavior for the 367-cm^{-1} band and acceptor behavior for the 369-cm^{-1} band, which is exactly counter to the identities of these centers being Si_{Ga}-Ga_{As} and Si_{As}-As_{Ga}, respectively, as indicated by the Green's-function calculations. A second problem is the apparent absence of the line (near 323 cm^{-1}) proposed in the theory but not found in the absorption spectrum. Careful irradiation and annealing investigations are therefore very much needed to clarify the above points. Finally, to accept the theoretical models

proposed for the 367- and 369-cm^{-1} bands, we believe that ir measurements regarding the influence of uniaxial compression will further help in assigning at least the symmetry of the defect centers.

ACKNOWLEDGMENTS

One of us (D.N.T.) is thankful to the Chairman of Department de Physico Chimie, Commissariat à l'Energie Atomique, Centre d'Etudes Nucléaires de Saclay, for providing him with an opportunity of working in the Services Chimie-moleculaire. The experimental measurements were performed at the United States Air Force Avionics Laboratory, Wright Patterson Air Force Base, Ohio, under Air Force Office of Scientific Research Contract No. AFOSR F33615-84-C-1423.

[1]A. G. Milnes, *Deep Impurities in Semiconductors* (Wiley, New York, 1973).
[2]A. M. Stoneham, *Theory of Defects in Solids* (Clarendon, Oxford, 1975).
[3]S. T. Pantelides, Rev. Mod. Phys. **50**, 797 (1978).
[4]M. Jaros, Adv. Phys. **29**, 409 (1980).
[5]R. C. Newman, *Infrared Studies of Crystal Defects* (Taylor and Francis, London, 1973).
[6]W. G. Spitzer, *Festkörperprobleme XI*, edited by O. Madelung (Pergamon, New York, 1971), pp. 1–44.
[7]A. S. Barker and A. J. Sievers, Rev. Mod. Phys. Suppl. **47**, S1 (1975).
[8]R. J. Wagner, J. J. Krebs, G. H. Stauss, and A. M. White, Solid State Commun. **36**, 15 (1980).
[9]T. A. Kennedy and N. D. Wilsey, Phys. Rev. Lett. **41**, 977 (1978); Phys. Rev. B **23**, 6585 (1981).
[10]G. D. Watkins, in *Defects and Radiation Damage in Semiconductors*, edited by J. E. White (IOP, London, 1973), p. 228.
[11]U. Kaufman, J. Schneider, and A. Rauber, Appl. Phys. Lett. **29**, 312 (1976).
[12]D. V. Lang, R. A. Logan, and L. C. Kimerling, Phys. Rev. B **15**, 4874 (1977).
[13]R. H. Wallis, A. Zylbersztejn, and J. M. Besson, Appl. Phys. Lett. **38**, 431 (1981).
[14]H. Temkin, B. V. Dutt, and W. A. Bonner, Appl. Phys. Lett. **38**, 431 (1981).
[15]W. M. Theis, K. K. Bajaj, C. W. Litton, and W. G. Spitzer, Appl. Phys. Lett. **41**, 70 (1982); Physica **117&118B**, 116 (1983).
[16]G. A. Gledhill, R. C. Newman, and J. Woodhead, J. Phys. C **17**, L301 (1984); W. J. Moore, B. V. Shanabrook, and T. A. Kennedy, Solid State Commun. **53**, 957 (1985).
[17]W. M. Theis, in *Spectroscopic Characterization Techniques for Semiconductor Technology II*, edited by Fred H. Pollak (SPIE, New York, 1985), Vol. 45, p. 524.
[18]B. V. Shanabrook, W. J. Moore, T. A. Kennedy, and P. P. Ruden, Phys. Rev. B **30**, 3563 (1984).
[19]K. Laithwaite and R. C. Newman, Philos. Mag. **35**, 1689 (1977).
[20]R. T. Chen and W. G. Spitzer, J. Electron. Mater. **10**, 1085 (1981).
[21]R. T. Chen and W. G. Spitzer, J. Electrochem. Soc. **127**, 1607 (1980).
[22]R. T. Chen, V. Rana, and W. G. Spitzer, J. Appl. Phys. **51**, 1532 (1980).
[23]R. C. Newman, F. Thompson, M. Hyliands, and R. F. Peart, Solid State Commun. **10**, 505 (1972).
[24]M. R. Brozel, J. B. Clegg, and R. C. Newman, J. Phys. D **11**, 1331 (1978).
[25]W. G. Spitzer and W. Allred, Appl. Phys. Lett. **12**, 5 (1968).
[26]L. H. Skolnik, W. G. Spitzer, A. Kahan, F. Euler, and R. G. Hunsperger, J. Appl. Phys. **43**, 2146 (1972).
[27]P. C. Leung, J. Fredrickson, W. G. Spitzer, A. Kahn, and L. Bouthilette, J. Appl. Phys. **45**, 1009 (1974).
[28]F. Thompson and R. C. Newman, J. Phys. C **5**, 1999 (1972); **5**, 2010 (1972).
[29]M. R. Brozel, R. C. Newman, and B. Ozbay, J. Phys. C **12**, L785 (1979).
[30]W. M. Theis and W. G. Spitzer, J. Appl. Phys. **56**, 890 (1984).
[31]F. Thompson, S. R. Morrison, and R. C. Newman, *Radiation Damage and Defects in Semiconductors* (IOP, London, 1973), p. 371.
[32]S. R. Morrison, R. C. Newman, and F. Thompson, J. Phys. C **7**, 633 (1974).
[33]S. R. Morrison and R. C. Newman, J. Phys. C **7**, 619 (1974).
[34]J. Woodhead, R. C. Newman, I. Grant, D. Rumsby, and R. M. Ware, J. Phys. C **16**, 5523 (1983).
[35]A. M. White, P. J. Dean, D. J. Ashen, J. B. Mullin, M. Webb, B. Day, and P. D. Greene, J. Phys. C **6**, L243 (1973); D. C. Reynolds, C. W. Litton, E. B. Smith, P. W. Yu, and K. K. Bajaj, Solid State Commun. **42**, 827 (1982).
[36]D. J. Ashen, P. J. Dean, D. T. J. Hurle, J. B. Mullin, A. M. White, and P. D. Greene, J. Phys. Chem. Solids **36**, 1041 (1975).
[37]R. S. Leigh and R. C. Newman, J. Phys. C **15**, L1045 (1982).
[38]P. Kleinert, Phys. Status Solidi B **119**, K37 (1983); **117**, K91 (1983); **124**, 559 (1984).
[39]A. A. Maradudin, E. W. Montroll, C. H. Weiss, and I. P. Ipatova, in *Solid State Physics*, 2nd ed., edited by F. Seitz, D. Turnbull, and H. Ehrenreich (Academic, New York, 1971).
[40]R. J. Elliott, J. A. Krumhansl, and P. L. Leath, Rev. Mod. Phys. **46**, 465 (1974).
[41]M. Vandevyver, D. N. Talwar, P. Plumelle, K. Kunc, and M. Zigone, Phys. Status Solidi B **99**, 727 (1980).
[42]K. Kunc, Physica **116B**, 52 (1983).
[43]A. Grimm, A. A. Maradudin, I. P. Ipatova, and A. V. Subashiev, J. Phys. Chem. Solids **33**, 775 (1972).
[44]D. N. Talwar and Bal K. Agrawal, Phys. Rev. B **12**, 1432 (1975).
[45]M. Vandevyver and P. Plumelle, Phys. Rev. B **17**, 675 (1978).
[46]M. Vandevyver and D. N. Talwar, Phys. Rev. B **21**, 3405 (1980).
[47]P. Plumelle, D. N. Talwar, M. Vandevyver, K. Kunc, and M. Zigone, Phys. Rev. B **20**, 4199 (1979).
[48]D. N. Talwar and Bal K. Agrawal, J. Phys. Chem. Solids **39**, 207 (1978).
[49]R. S. Leigh and M. J. L. Sangster, J. Phys. C **15**, L317 (1982).
[50]D. N. Talwar, M. Vandevyver, and M. Zigone, J. Phys. C **13**, 3775 (1980); Phys. Rev. B **23**, 1743 (1981).
[51]J. L. T. Waugh and G. Dolling, Phys. Rev. **132**, 2410 (1963).
[52]K. Kunc, Ann. Phys. (Paris) **8**, 319 (1973–74).
[53]J. deLaunay, in *Solid State Physics*, edited by F. Seitz, D. Turnbull, and H. Ehrenreich (Academic, New York, 1956), 1956), Vol. 2, p. 210.
[54]R. M. Feenstra, R. J. Hausenstein, and T. C. McGill, Phys. Rev. B **28**, 5793 (1983).

[55]J. F. Angress, G. A. Gledhill, and R. C. Newman, J. Phys. Chem. Solids **41**, 341 (1980).
[56]O. H. Nielsen, Ph.D. thesis, Institute of Physics, University of Aarhus, 1981 (unpublished).
[57]D. N. Talwar, Ph.D. thesis, Allahabad University, 1976 (unpublished).
[58]J. P. Walter and M. L. Cohen, Phys. Rev. B **4**, 1877 (1971).
[59]J. Chelikowsky and M. L. Cohen, Phys. Rev. B **14**, 556 (1979).
[60]W. A. Harrison, *Electronic Structure and the Properties of Solids* (Freeman, San Francisco, 1980).
[61]G. A. Baraff, E. O. Kane, and M. Schlüter, Phys. Rev. B **25**, 548 (1982).
[62]J. A. Van Vechten, *Handbook on Semiconductors,* edited by T. S. Moss and S. P. Keller (North-Holland, Amsterdam, 1980), Vol. 3, pp. 1—111.
[63]N. K. Goswami, R. C. Newman, and J. E. Whitehouse, Solid State Commun. **40**, 473 (1981).
[64]R. C. Newman, in *Festkörperprobleme* (*Advances in Solid State Physics*), edited by P. Grosse (Vieweg, Braunschweig, 1985), Vol. XXV, p. 605.
[65]S. P. Gaur, J. F. Vetelino, and S. S. Mitra, J. Phys. Chem. Solids **32**, 2737 (1971).
[66]L. Bellomonte, J. Phys. Chem. Solids **38**, 59 (1977).